



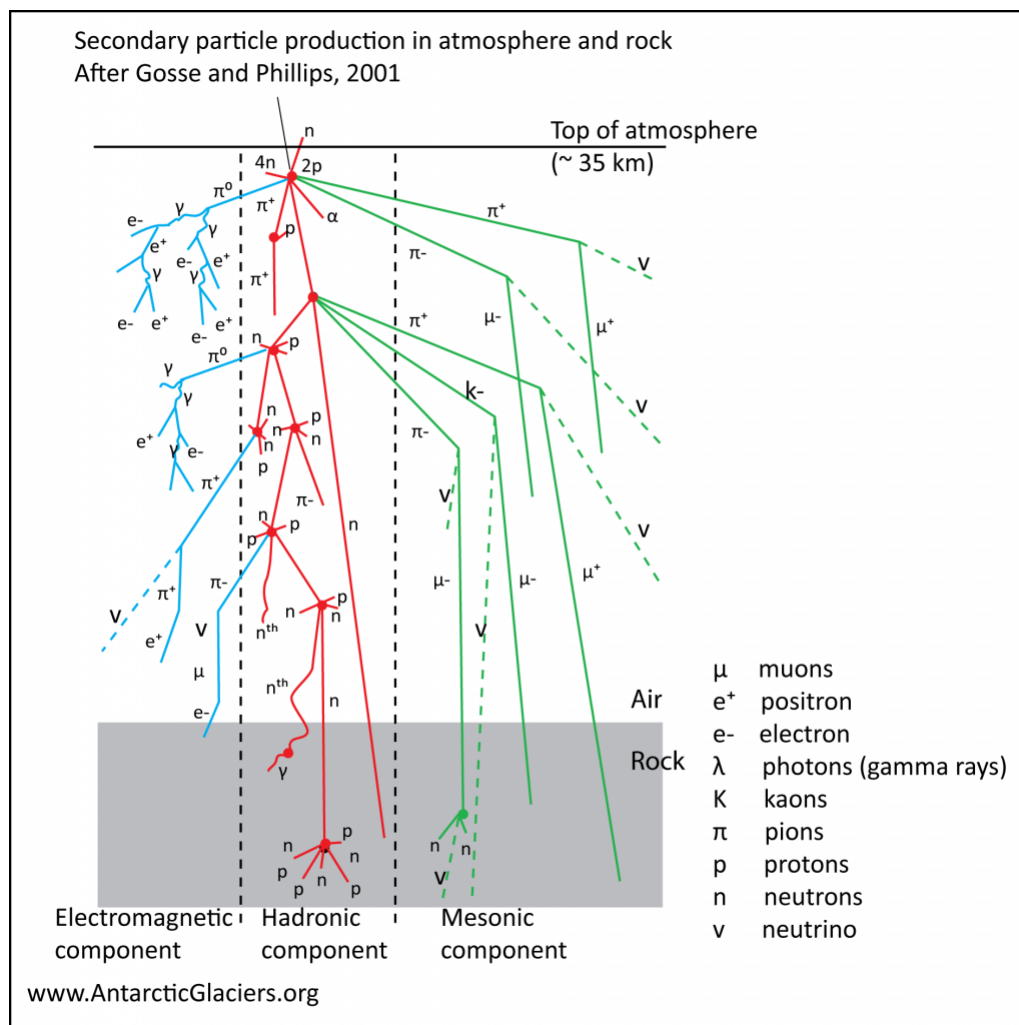
Production of cosmogenic nuclides

This article is edited and drawn from:

Davies, B.J., 2022. Dating Glacial Landforms II: Radiometric Techniques, in: Haritashya, U. (Ed.), Treatise in Geomorphology (Second edition). Cryospheric Geomorphology. Elsevier, pp. 249-280. ([link](#))

Bombardment by solar radiation

Cosmogenic nuclides are being constantly formed. The Earth is continuously bombarded from all directions by cosmic radiation (Balco, 2011; Dunai and Lifton, 2014; Gosse and Phillips, 2001). These [cosmic rays](#) largely originate from Supernova explosions from the galaxy and beyond our Solar System, and, at the top of our atmosphere, comprise high-energy protons (87%), alpha particles (12%) and heavy nuclei (1%). When these high-energy particles enter our atmosphere, these primary cosmic rays interact with atoms to produce secondary cosmic rays.

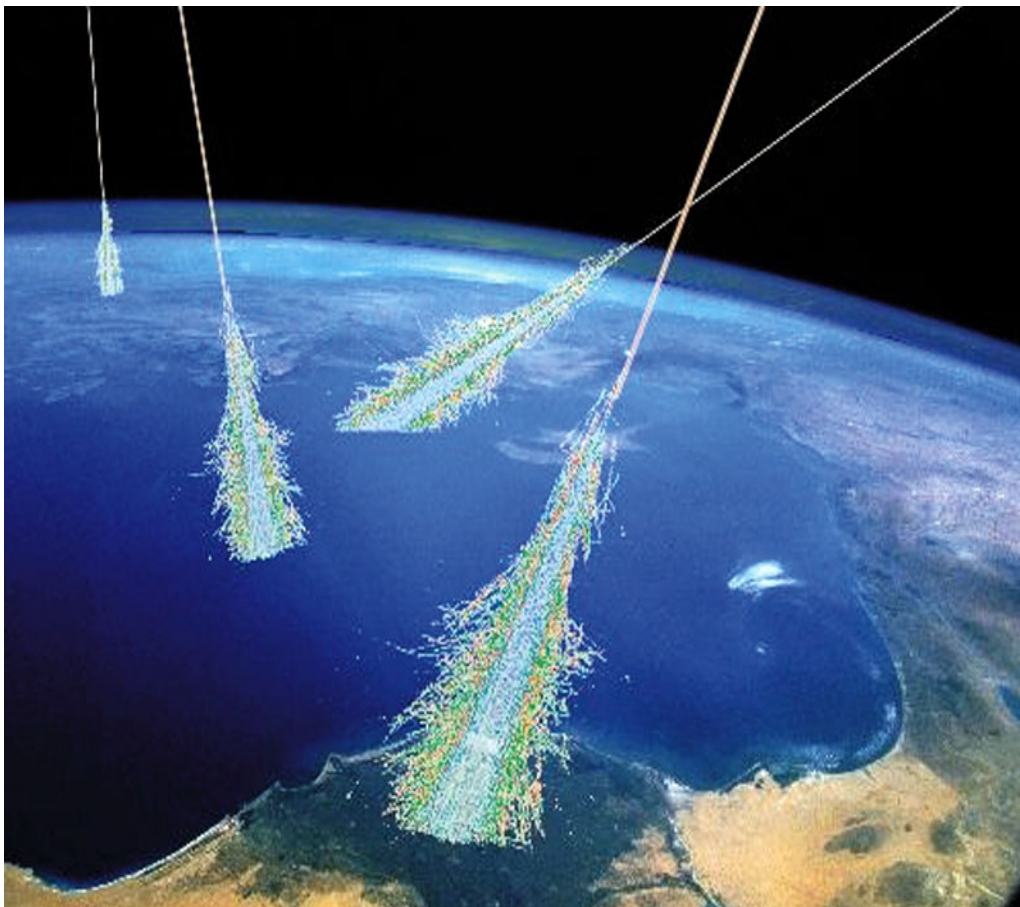


The cosmic ray cascade. Spallation reactions cause the formation of new cosmogenic nuclides in the atmosphere and in the lithosphere.

Spallation

The high-energy primary cosmic rays are in excess of the binding energies of atomic nuclei. Spallation is a reaction that occurs when nucleons are sputtered off target nuclei following the collision of a primary cosmic ray with a target atom (Dunai and Lifton, 2014). This leaves behind a lighter residual nucleus, such as those shown in Table 2.

These spallation-induced nuclei continue in the same direction as the primary cosmic ray, and retain sufficient energy to continue to induce spallation reactions in other target minerals. This results in a nuclear cascade through the Earth's atmosphere, forming meteoric ^{14}C , ^{10}Be , and other cosmogenic nuclides. Energy lost with each interaction means that the mean energy of the secondary neutron flux at sea level is substantially lower than that of the primary flux (Dunai and Lifton, 2014).



The cosmic ray shower. It is now known that most cosmic rays are atomic nuclei. Most are hydrogen nuclei, some are helium nuclei, and the rest heavier elements. The relative abundance changes with cosmic ray energy — the highest energy cosmic rays tend to be heavier nuclei. Although many of the low energy cosmic rays come from our Sun, the origins of the highest energy cosmic rays remains unknown and a topic of much research. This drawing illustrates air showers from very high energy cosmic rays. Image from NASA.

The collisions in the upper atmosphere also produce negatively charged muons. They have a greater penetration depth than nucleons, and interact only weakly with matter (Dunai and Lifton, 2014). They are the most abundant cosmic ray particles at sea level. However, spallation reactions with the nucleonic component dominate atmospheric and terrestrial cosmogenic nuclide production ([Table 2](#)).

Eventually, the neutrons in the nuclear cascade slow down to energies corresponding to the temperature of their surroundings (Dunai and Lifton, 2014). These “thermal neutrons” can then be captured by nuclei. In some cases (^3He , ^{36}Cl), this is an important production source for cosmogenic

nuclides.

Formation of terrestrial cosmogenic nuclides

Terrestrial cosmogenic nuclides are therefore produced in rocks by these interactions between secondary cosmic radiation and minerals at the Earth's surface. The six most commonly used cosmogenic isotopes, which have well-established production rates at the Earth's surface that are large enough to be measured, and long-enough half-lives to be useful, are listed in [Table 2](#).

Cosmogenic nuclide	Main target elements	Applicable rocks and minerals	Reactions	Half-life	Applicable time range	Production rate (LSD Sa scaling scheme)
³ He	Many, including Li	Olivine, pyroxene	Spallation (100%) Thermal neutron capture (on Li via ³ H)	Stable	To millions of years	Quartz: 114.55
²¹ Ne	Mg, Al, Si	Quartz, olivine, pyroxene	Spallation (>96.4%)	Stable	Tens of thousands to millions of years	
¹⁰ Be	O, Si	Quartz (sandstones, granites, gneisses, etc.)	Spallation (96.4%) Muons (3.6%)	1.36 Ma	Ages from hundreds to several million years	Quartz: 3.92
²⁶ Al	Si	Quartz (sandstones, granites, gneisses, etc.)	Spallation (95.4%) Muons (4.6%)	0.7 Ma	Ages to several million years	Quartz: 28.54
³⁶ Cl	K, Ca, Cl (Fe, Ti)	All rock types. Basalts; volcanic rocks; limestones and carbonate rocks	Thermal neutron capture (from Cl and K) Muons (4.6% from K; 13.4% from Ca)	0.3 Ma	To one million years	Ca: 56.27 K: 156.09
¹⁴ C	O, Si	Quartz (sandstones, granites, gneisses, etc.)	Spallation (82%) Muons (18%)	5.73 ka	To 20,000 years	Quartz: 12.76

Table 2. Major cosmogenic nuclides used in geomorphological research, their target elements and minerals, reaction pathways and production rates. Multiple sources (Borchers et al., 2016; Darvill, 2013; Dunai, 2010; Granger et al., 2013; Ivy-Ochs and Kober, 2007; Nishiizumi et al., 2007). Global production rates are given in atoms per gram per year, after Borchers et al. (2016). Table from Davies, 2022

Beryllium-10 in Quartz

Of these isotopes, ¹⁰Be is used most widely to date glacial landforms such as moraines (Granger et al., 2013). This is because its production rate has been well studied and calibrated (Balco et al., 2009; Borchers et al., 2016; Kaplan et al., 2011; Putnam et al., 2010; Small and Fabel, 2015), and because it forms easily from Si and O in quartz, a widespread and common mineral at the Earth's surface. Quartz is resistant to weathering, ubiquitous, and has a simple stoichiometric chemistry (Gosse and Phillips, 2001).

For this reason, glacially transported felsic phaneritic rocks (granites) are often targeted for exposure age dating. Granites are resistant to weathering and durable, and can be transported long distances. ^{10}Be also has a long half-life, making it useful for long exposures. ^{10}Be has routinely good precision in AMS measurements, a standardized chemistry procedure (Nishiizumi et al., 2007), and the isotope ^9Be is rare in quartz, making it simpler to measure (Granger et al., 2013).



Alan Hill sampling a large granite boulder for ^{10}Be exposure-age dating. Photo credit: Bethan Davies

Using ^{10}Be to date moraines

^{10}Be has been used to date glacial landforms from the mid-Pleistocene (e.g., Hein et al., 2017, 2009; Mendelová et al., 2020). It has also been applied to date young moraines that date from the last few hundred years in temperate environments (e.g., Kaplan et al., 2016; Schaefer et al., 2009; Schimmelpfennig et al., 2014).

Challenges for ^{10}Be dating include that atmospheric ^{10}Be is a significant source of contamination, so quartz grains must be etched and cleaned in the measurement process (Gosse and Phillips, 2001).

Using other cosmogenic isotopes

^{10}Be can be paired with ^{26}Al , which can highlight inheritance issues (Bentley et al., 2006; Fabel et al., 2002). Both isotopes form in quartz, but have different half-lives. The divergence of the two isotopes can be an indicator for prior exposure. The production rate of ^{26}Al is higher than that of ^{10}Be (Table 2). It can be difficult to measure low $^{26}\text{Al}/^{27}\text{Al}$ in quartz with high Al contents (Gosse and Phillips, 2001).

^{14}C can be applied to shorter chronologies (> 30 kyr), especially to Holocene glacial histories (Goehring et al., 2011). The short half-life makes it applicable where erosion rates are low and inheritance may be an issue (Gosse and Phillips, 2001; Miller et al., 2006; White et al., 2011), or exposure histories may be complex (Goehring et al., 2013). It is suitable for quartz-bearing rocks, and can be paired with ^{26}Al and ^{10}Be (Hippe et al., 2014; White et al., 2011), but potential contamination can make sample preparation difficult and expensive (Lifton et al., 2001).

^{36}Cl can be used on a range of lithologies, and is often used on volcanic rocks and basalts that are low in quartz, prohibiting ^{10}Be dating (Briner et al., 2001; Çiner et al., 2015; Sarkaya et al., 2017; Schimmelpfennig et al., 2009). However, production rates are less well constrained than those for ^{10}Be , because the multiple pathways for production on multiple elements are difficult to decipher (Gosse and Phillips, 2001; Marrero et al., 2016b).

^3He has a high production rate and low detection limit in a conventional AMS, so can be used to date younger exposure ages. As it is stable, it can also be used to date longer exposure ages (Goehring et al., 2010). ^3He can be used to date lavas without quartz (e.g., Espanon et al., 2014; Johnson et al., 2009). The availability of well-preserved lava flows with independent age control means that production rates are well distributed spatially (Goehring et al., 2010).

The production rate is better quantified than for ^{21}Ne (Gosse and Phillips, 2001). However, it diffuses rapidly in quartz and fine-grained groundmass in aphanitic rocks, and a correction for radiogenic, nucleogenic and magmatic ^3He is necessary. There is also a greater risk of inheritance as it is a stable nuclide.

^{21}Ne is suitable for dating extremely long exposures, because it is stable (Gosse and Phillips, 2001). This does mean that inheritance may be more of an issue for this isotope. A correction of radiogenic or nucleogenic ^{21}Ne is required.

Production Rate

The *production rate* calculates the rate that a particular cosmogenic nuclide is produced at the sampling site. It is expressed in units of atoms produced per year per gram of target material (Borchers et al., 2016). The *in situ* production rate varies according to latitude, altitude, and the thickness and density of a sample (Darvill, 2013; Dunai, 2000; Lal, 1991; Stone, 2000).

Production rates are nuclide-specific and can be established regionally using independently dated features such as radiocarbon-dated moraines (Balco et al., 2009; Kaplan et al., 2011; Putnam et al., 2010), varved records with tephra (Small and Fabel, 2015), argon-dated volcanic lavas (Foeken et al., 2012), or tree-ring chronologies (Kubik et al., 1998). Published production rates are normalized to sea-level and high-latitude (SLHL), and then must be scaled using a *scaling scheme* according to altitude and latitude (Borchers et al., 2016). Global production rates are provided by Borchers et al. (2016) ([Table 2](#)). Generally, production rates should be applied locally and compared with global production rates. Production rates for ^{10}Be are best quantified. Some examples of local production rates are shown in [Table 3](#).

ICE-D (Informal Cosmogenic-nuclide Exposure-age Database; <http://ice-d.org>) is a production rate database that includes published empirical calibration rate studies (Balco, 2020; Martin et al., 2017). This allows the user to select a global, regionally averaged or local production rate for age calculation. It is compatible with several cosmogenic nuclide calculators, including CRONUS-calc.

Location	Reference	^{10}Be production rate (atoms/g/yr)	Comments and scaling scheme	Calibration method
Global	Borchers et al. (2016)	3.92	LSDn (Sa) scaling scheme	Analysis of global datasets
Patagonia	Kaplan et al. (2011)	3.71 ± 0.11	When using a time-dependent scaling method that incorporates a high resolution geomagnetic model.	Independently dated moraines (^{14}C)
Southern Alps, New Zealand	Putnam et al. (2010)	3.74 ± 0.08	Using 'Lm' scaling scheme. Relative to '07KNSTD'	Independently dated moraines (^{14}C)
Scotland	Small and Fabel (2015)	4.26 ± 0.21	Using 'Lm' scaling scheme	Glacial lake shorelines independently dated with varves and tephra
North America	Balco et al. (2009)	4.26 ± 0.21	Using 'Lm' scaling scheme	Independently dated Late Glacial landforms
Scandinavia	Stroeven et al. (2015)	4.13 ± 0.11	Using 'Lm' scaling scheme	Varved lake sediments
Scandinavia	Stroeven et al. (2015)	3.95 ± 0.10	Using 'LSDn' scaling scheme	Varved lake sediments

Table 3. Examples of regional production rates for ^{10}Be , scaled to SLHL. For a complete database, the reader is referred to ICE-D. From Davies, 2022

Downloaded from:

<https://www.antarcticglaciers.org/glacial-geology/dating-glacial-sediments-2/cryospheric-geomorphology-dating-glacial-landforms/cosmogenic-nuclide-dating-cryospheric-geomorphology/production-of-cosmogenic-nuclides/>